UV Index: trend and maximum values from hourly measurements during twenty years (2000-2019) over the Mexico City Metropolitan Area

Adriana Ipiña[1], Gamaliel López-Padilla[2], Rubén D Piacentini[1], and Sasha Madronich[3]

[1]Instituto de Física Rosario (CONICET-UNR), Rosario, Argentina
[2]Facultad de Ciencias Físico Matemáticas, Universidad Autónoma de Nuevo León, San Nicolás de los Garza, México
[3]National Center for Atmospheric Research, Boulder, Colorado USA

October 27, 2020

Abstract

The UV Index is a measure of the risk of suffering erythema from short-term solar exposure. Mexico City is one of the most populated cities in the world, and could experience large exposures due to its location at 2240 m above sea level, and its intertropical latitude. In the present study we analyzed around 2 million ground-based UV Index measurements from the Secretariat of the Environment of the Mexico City Government during two decades (2000-2019) over the Mexico City Metropolitan Area. An increasing trend in the UV Index, of 0.66 % per year was found. Trends in criteria pollutants PM_{10}, CO, NO_2, O_3 and in AOD_{340} were also estimated. The monthly mean UV Index value at solar noon reaches barely 10.5 under all sky conditions, along the year. UV Index data derived from OMI-Aura/NIVR-FMI-NASA measurements of ozone and clouds ranged between 6.4 and 14.9. The UV Index was used to estimate the Standard Erythema Dose (SED) per hour for high sun under clear sky conditions, and from these we estimate exposure times as a limit to avoid sunburn for typical skin phototypes (III and IV of the Fitzpatrick classification) in Mexico City. These results may be helpful to design preventive public health campaigns that target groups with typical phototypes of the inhabitants of the Mexico City.

Keywords: UV Index, Solar UV radiation, Mexico City, Skin Phototypes, Standard Erythemal Dose.

Introduction

Mexico City is the largest city in North America by number of inhabitants and one of the largest urban agglomeration in the world (UN, 2014). The latitude and longitude coordinates for the city are 19.4°N and 99.1°W, at an average height of 2240 meters above sea level. The Mexico City Metropolitan Area (MCMA) is surrounded by mountain ridges exceeding 5000 m asl and has been the subject of multiples studies related to air quality due to intense anthropogenic activity (Doran et al., 1998; Molina et al., 2007; Molina et al., 2010; Tzompa-Sosa et al., 2017). The complex topography and thermal inversions inhibit winds that sweep away pollution and influence the surface energy balance (Whiteman et al., 2000; Tejeda-Martínez and Jáuregui-Ostos, 2005; Zhang et al., 2009). Solar radiation varies along the hours of the day and the days of the year, as well as via its dependence of atmospheric components that attenuate the different wavelengths. The ultraviolet (UV) range is only a small part of total incident irradiance, but plays a key role in atmospheric photochemistry (Leighton, 1961; Seinfeld and Pandis, 2016). On the pathway through the atmosphere, photons experience scattering by air molecules, aerosol particles (haze) and clouds, as well as absorption by gases such as ozone (O_3) and nitrogen dioxide (NO_2), and some aerosols. An increase in ozone concentration

in polluted boundary layers is also generated by strong UV photon fluxes interacting with anthropogenic precursor emissions (Leighton, 1961; Finlayson-Pitts and Pitts, 2000). Conversely, aerosols may increase or reduce the insolation and photolysis rates, and thus affect photochemical smog formation (Dickerson, 1997). A modelization of actinic flux applied to Mexico City, showed a decrease at the surface and an increase aloft, mainly due to the presence of aerosols (Palancar et al., 2013). Likewise, a reduction in the measured and theoretical values of nitrogen dioxide photolysis rate was attributed to attenuation of spectral actinic solar flux by aerosols (Castro et al., 2001).

Despite multiple efforts to monitor and characterize air quality in the Mexico City basin, few studies have specially focused on global solar radiation (Galindo et al., 1991; Quiñones and Almanza, 2014; Matsumoto et al., 2014). In the mid-1990s, two studies about UV solar irradiance measurements in the Mexican Valley, for periods shorter than 3 years, were published. One of these studies suggested a significant attenuation on UV intensity due to tropospheric ozone, comparing measurements in downtown and outskirts of the Mexico City (Acosta and Evans, 2000). Another study reported that Mexico City had lower ultraviolet fluxes (around 25% at noon and 50% in the afternoon) compared to Colima, a city placed at the same latitude, lower elevation (ca. 300-500 m asl) and almost pollution-free. (Galindo et al., 1995). To our knowledge, these are the only published long-term measurements of UV radiation in Mexico City. Short-term measurements and comparisons with radiative models were reported by (Palancar et al., 2013). Other UV measurements have been carried out to estimate aerosol optical properties at UV wavelengths, e.g. using UV Multi-Filter Rotating Shadowband Radiometers (MFRSRs) to estimate aerosol single scattering albedo (Goering, 2005; Corr et al., 2009), but did not focus on the UV Index.

UV Index (UVI) is an indicator related to the intensity of the solar UV radiation at the Earth's surface and the risk for persons to suffer sunburn, and may be relevant to chronic effects due to prolonged exposure, such as skin cancer. Fitzpatrick classification defines six phototypes (I-VI) or skin colors from pale to dark, correlated to the UV radiation sensitivity (Fitzpatrick, 1974). The International Commission on Illumination (CIE) established an action spectrum for erythema (or erythemal sensitivity) of human skin using phototype II from Fitzpatrick classification (CIE, 2014). According to the World Health Organization (WHO) the UVI is expressed mathematically as follows:

$$UVI = \int_{250nm}^{400nm} k_{er} \cdot E(\lambda, t) \cdot S_{er}(\lambda)\, d\lambda \tag{1}$$

where $E(\lambda, t)$ is the solar spectral irradiance in units of W/(m^2 ·nm), $S_{er}(\lambda)$ is the erythemal sensitivity defined by CIE and k_{er} is a factor equal to 40 m^2/W. The WHO standarized the UVI scale as: low (0, 1 and 2), moderate (3, 4 and 5), high (6 and 7), very high (8, 9 and 10) and extreme (11 or more) (WHO, 2002). Even values of UVI above 20 have been recorded in La Quiaca, Argentina (Cede et al., 2002). An extended recommendation of the WHO version is unfolding UVI values larger than 11 and modifying the color scale (Zaratti et al., 2014). This suggestion could be appropriate for the Mexico City due to UVI reaching values considered as high, almost all year in this latitudinal band (Tanskanen et al., 2006; Herman, 2010). The skin reddening (or erythema, as a sign of possible sunburn or even more complicated skin diseases (Fitzpatrick, 1974)) caused by solar radiation depends on intensity of the source, skin phototype and exposure time. For an interval time $(t_2 - t_1)$ the erythemal dose or erythemal radiant exposure (Braslavsky, 2007) is calculated as:

$$H_{er} = \int_{t_1}^{t_2} E_{er}(t)\, dt = \int_{t_1}^{t_2} \frac{1}{k_{er}} \cdot UVI \tag{2}$$

where the term $E_{er}(t)$ is the erythemal irradiance obtained from $\frac{1}{k_{er}} \cdot UVI$. The H_{er} value, when applied to each skin phototype, predicts the appearance of erythema some hours after exposure. For example, minimal erythema in skin type II requires a dose between 250-300 J/m^2 (Fitzpatrick, 1988; Molina et al., 2010; Pérez et al., 2014; Lehmann et al., 2019). This H_{er}value to produce erythema was established as the Minimal Erythemal Dose (MED), which has been widely used as a primary and preventive measure of skin damage. Several studies have examined values of MED for different skin phototypes (MacKie, 2000; Meinhardt et al.,

2008; Miller et al., 2012). CIE proposed the Standard Erythemal Dose (SED) with a value of 100 J/m^2 as an erythemally weighted unit dose, independent of skin phototype (CIE, 2014). So, H_{er} can be calculated for each skin phototype, in units of SEDs. The lowest values of the MED ranges defined by Fitzpatrick under UVB radiation for each phototype, are taken as reference in this work (see Table 1, (Fitzpatrick, 1988)).

Skin cancer is one of the most damaging effects of long-term solar exposure and is very common in most regions the world, according to the World Health Organization (WHO, 2002). In Mexico, the incidence is probably under-reported since the majority of skin cancers are not cause of death (Jurado-Santa-Cruz et al., 2011). While melanoma is a primarily risk on fair skins, long-term exposure is believed to induce melanoma in latino population as well mainly those working in outdoor conditions (Rouhani et al., 2008).

There are few publications about the epidemiology of skin cancer produced by solar exposure in Latin America, and even fewer about incidence and mortality rates related to ethnic origin (see for instance (de Vries et al., 2016)). Notwithstanding the high UV Index levels reported in other regions of the country (Castanedo-Cázares et al., 2012), a percentage of the Mexican population still uninformed about the harmful effects of prolonged exposure under the sun (Castanedo-Cazares et al., 2006). Skin types in Mexico derive from wide mixing of ethnic groups. In multiple studies, notions about the variety of skin colors are often associated to 'race', 'ethnic skin' or 'Hispanic skin' (Taylor et al., 2005; Bino and Bernerd, 2013; Robinson et al., 2017). Terminology to describe the origin, such as: Latinos of Mexican heritage, Mexican-American, Latin American or Hispanic involves a genetic background, cultural traditions and customs, that would dictate a degree of caution for the people who would otherwise, based on nationality or appearance alone, would be classified as of low-risk sensitivity (de Vries et al., 2016; Wolbarsht and Urbach, 1999; Lancer, 1998; Bino and Bernerd, 2013). Nonetheless, these labels may accentuate the problem of inadequate generalization (Cuevas et al., 2016; Marcheco-Teruel et al., 2014). A specific publication about this topic concluded that "skin color" is a term and a concept that is relevant to cutaneous biology and disease research, independent of racial background (Torres et al., 2017). This argument supports the choice of Fitzpatrick convention for this study, excluding ethnic terminology to calculate the erythemic dose thresholds (H_{er}) according to skin color.

Regarding to the skin appearance, the last edition of the National Survey About Discrimination (ENADIS) using the methodology of the PERLA (Latin American Race and Ethnicity Project), published information related to skin type of the Mexican population on a palette of 11 colors (ENADIS, 2017). An adaptation of these skin colors grouped into Fitzpatrick phototypes and their respective percentages present in Mexican people, are displayed in Table 1. Since the largest fraction (83.2%) of the people has phototype in the color ranges III (24.0%) and IV (59.2%) in the country, we take into account these types as representative to calculate the maximum exposure times to avoid sunburn, of course with the understanding that paler colors require shorter times and darker ones need longer times to generate sunburn.

Some reports have indicated that outdoor workers receive between 10% and 80% of ambient UV radiation (Larkö and Diffey, 1983; Makgabutlane et al., 2015; Silva, 2016; Moldovan et al., 2020). With over 21 million persons living in the MCMA, exposure to solar UV radiation constitutes a major public health issue. In this intertropical zone, intense UV radiation is present in a wide daylight window almost all year, so that the UV Index is a useful and indispensable reference to prevent unwanted skin exposure. The assessments of the UV irradiance contribute to the knowledge of the regional climatology as well as the global monitoring of the atmosphere (Madronich, 1993; Fioletov et al., 2004; Staiger and Koepke, 2005; Luccini et al., 2006; Herman, 2010; Utrillas et al., 2018). Likewise, a lot of scientific publications around the world describe the importance of understanding the UV irradiance behavior along the time and its relation with the MED (Rivas et al., 2011; Rivas et al., 2015; Lehmann et al., 2019; Parra et al., 2019; Cadet et al., 2019). Despite of the relevance of UVI as a communication tool in relation to the public health, at present there are no studies focused on the maximum values attained and its behavior in Mexico City. The aim of this work is to analyze twenty years of UV Index measurements over MCMA to determine: trends, averages and maximum values as well as values filtered under cloudless sky. Finally, the SED/hr is calculated to quantify the solar exposure times to accumulate the (H_{er}) for 1 MED on skin phototype III and IV.

Phototype	H_{er} (SED)	Skin color	skin color of the Mexican population (%)
I	2.0		0.8
II	2.5		3.9
III	3.0		24.0
IV	4.5		59.2
V	6.0		8.9
VI	10.0		2.5

Table 1: Skin phototypes with their respectives minimal erythemal doses in terms of SED (Fitzpatrick, 1988) and adaptation from ENADIS study for the skin colors and their percentages (%) of presence in the Mexican population (ENADIS, 2017) grouped by phototype.

Measurement methodology

Ground-based

United Mexican States is in the latitudinal fringe 14.53°N - 32.71°N of the Americas, where its capital (Mexico City) lies in a basin 70 km northwest from Popocatepetl volcano, one of three highest peaks of the country with an altitude nearby 5426 m asl. The Secretariat of the Environment of the Mexico City Government (SEDEMA) of the Atmospheric Monitoring System (SIMAT) is in charge of the air quality monitoring in the Mexico City Metropolitan Area (Figure 1).

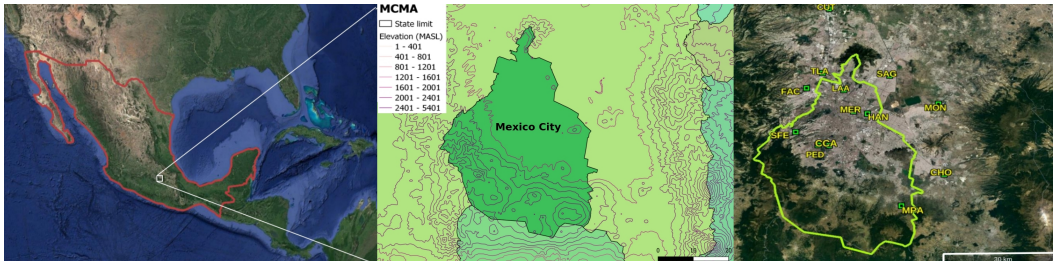

Figure 1: Maps from left to right: United Mexican States (red contour), Contour lines scale of Elevation over Mexican Valley (green area) and Distribution of the stations of the Atmospheric Monitoring System of Mexico City Government (green contour). Source: Figures at left and right, Google Earth. Figure at middle, base on CONABIO data (www.conabio.gob.mx/informacion/gis/) and QGIS.

Mexico City has a temperate climate with an extended wet season, although the rainfall is relatively high between June and August. The MCMA is in the North American Central Time Zone (CT) and uses the Central Standard Time (CST) i.e. six hours behind Coordinated Universal Time (UTC). In early spring, the local time changes five hours behind UTC due to the daylight saving time.

Since the year 2000, UV radiometers installed at the SIMAT network stations have been measuring erythemally-weighted solar radiation. These instruments are Model 501-A manufactured by Solar Light Company (SCL) with sensors detecting wavelengths between 280-400nm. The calibrations were carried out every year, using a reference sensor by the same manufacture. Although at the beginning only a few stations were in operation and have been changing, currently 11 stations are recording solar erythemal irradiances, which are converted to UV Indices, as given in Equation 1. The station names are: Chalco (CHA), Cuautitlán (CUT), FES Acatlán (FAC), Hangares (HAN), Laboratorio de Análisis Ambiental (LAA), Merced (MER), Montecillo (MON), Milpa Alta (MPA), Pedregal (PED), San Agustín (SAG), Santa Fe (SFE), Centro de Ciencias de la Atmósfera (CCA) and Tlalnepantla (TLA). The radiometers of the SIMAT have been

distributed over MCMA, prioritizing the sites with more density of population, as it is shown in Figure 1 right. The coordinates of the stations conforming the radiometers network are described in Table 2. On the SIMAT website http://www.aire.cdmx.gob.mx/default.php, UV Index measurements for each station are available almost in real time.

Even if there is no SLC radiometer at the station of the Centro de Ciencias de la Atmósfera (CCA) that belongs to the SIMAT, it has a photometer of the AErosol RObotic NETwork (AERONET see (Holben et al., 1998)). This instrument measures in situ the Aerosol Optical Depth (AOD) at 340nm. Additionally, we include measurements from the Automated Atmospheric Monitoring Network (Red Automática de Monitoreo Atmosférico, RAMA), a SIMAT subdivision, that is in charge of assessing the air quality. These dataset were used to perform a brief analysis about the criteria pollutants recorded by RAMA: Ozone (O_3), carbon monoxide (CO), nitrogen dioxide (NO_2) and concentration of particles with diameter less or equal than 10 μm (PM_{10}). The O_3 and NO_2 are reported in parts per billion (ppb), using ultraviolet photometry (Teledyne API model 400E) and chemiluminescence (Teledyne-API model 200E) respectively. The CO in parts per million (ppm) is derived by absorption of infrared light in a correlation cell (Teledyne API model 300E) and PM_{10} (in microgram per cubic meter) is measured by the beta attenuation method (Thermo Model 1405-DF FDMS).

Station	Environment	Lat (°N)	Lon (°W)	El (masl)
CHO	school zone	19.27	99.89	2253
CUT	ecological park	19.72	99.20	2263
FAC	urban	19.48	99.24	2299
HAN	urban	19.42	99.08	2235
LAA	urban	19.48	99.15	2255
MER	downtown	19.42	99.12	2245
MON	rural	19.46	98.90	2252
MPA	rural	19.18	98.99	2594
PED	residential	19.33	99.20	2326
SAG	urban	19.53	99.03	2241
SFE	residential	19.36	99.26	2599
TLA	urban	19.53	99.20	2311
CCA	University city	19.33	99.18	2294

Table 2: Abbreviations names, environmental descriptor and geographical position of the SIMAT stations placed in MCMA.

The available data set is rather larger, spanning two full decades for 5 stations and many years for the others, and with a measurement frequency of about 1 minute, thus resulting in ca. 2 million data points. Accordingly, significant averaging was carried out to highlight the main features of the data.

Satellite data

Satellite measurements of the Radiative Cloud Factor, the Total Ozone Column (TOC) and UV Index were used for the current study. These data were provided by the Ozone Monitoring Instrument (OMI) on board of AURA-NASA satellite and the Total Ozone Mapping Spectrometer (TOMS) on board the Earth Probe (EP)-NASA satellite. OMI was created in a cooperation between the Netherlands Agency for Aerospace Programmes (NIVR), the Finnish Meteorological Institute (FMI) and NASA. OMI (hereafter OMI-Aura/NIVR-FMI-NASA) performs observations over a geographical dimension of $13 \times 24\text{km}^2$ at nadir. For Mexico City, the satellite overpass time is between 19:00h - 21:00h UTC and data are specific for the coordinates and elevation of Mexico City. The TOMS-EP/NASA satellite instrument was also considered to complete the examined period. It is a version that precedes OMI and it was retrieving the TOC from spectral UV measurements.

Measurements analysis

Criteria pollutants: Ground-based measurements of PM_{10}, CO, O_3 and NO_2 from 11h to 14h CST were extracted from the SIMAT data to compute the daily averages at solar noon and the absolute maximums.

Aerosol Optical Depth: The AERONET Aerosol Optical Depth at 340 nm (AOD_{340}) data Product Level 2.0 were selected. The annual averages AOD_{340} were calculated from the continuous measurements during at least 7 months.

Cloud Factor and Total Ozone Column: The Radiative Cloud Factor and TOC derived from OMI-Aura/NIVR-FMI-NASA, for the OMTO3 v8.5 dataset, Collection 3 and L2 quality were collected. The Cloud Factor is dimensionless, from 0 to 1 for the cloudless days and overcast sky, respectively. TOC data were obtained from TOMS-EP/NASA. The 1461 observations were acquired of the: TOMS-EP/NASA instrument during the period 2000 to 2003 and OMI-Aura/NIVR-FMI-NASA data from 2004 to 2019, both dataset covering the complete time series of the ground-UV Index measurements.

UV Index: We developed a general code in `Python` to process the hourly averaged UV Index, 24 hours per day, 365 days a year, along two decades. Hereinafter, we refer to hourly averages simply as UV Index unless otherwise specified. The script also identifies the maximum UV index and ignores empty spaces and invalid values, product of the maintenance of the equipment. The algorithm creates a matrix with the maximum UV Index ($UVI_{\max}$) values sorted by date, hour and years. It selects the highest UV Index values of the network and a counter as an extension of the code was executed to quantify the values and their percentage frequency during 2000-2019 period. Thereupon it also calculates the hourly, monthly and annual averages. In particular, the values from 11h to 14h CST were isolated to compute the daily averages around solar noon and the absolute maximums. For the UV Index calculated from OMI-Aura/NIVR-FMI-NASA, we take into account all available daily values in the period 2000-2019 under the same specification of the Cloud Factor and TOC data.

Results and Discussion

The daily $UVI_{\max}$ were selected in the time interval 11:00 h-14:00 h CST from all ground-based measurements over MCMA. The results indicated that, from a total of 7305 days of continuous measurements, the daily UVI_{max} reached values between 6 and 9 on 62.37% of the days (Figure 2). The highest UV Index values were in the 13-14 range, with a frequency of less than 1%.

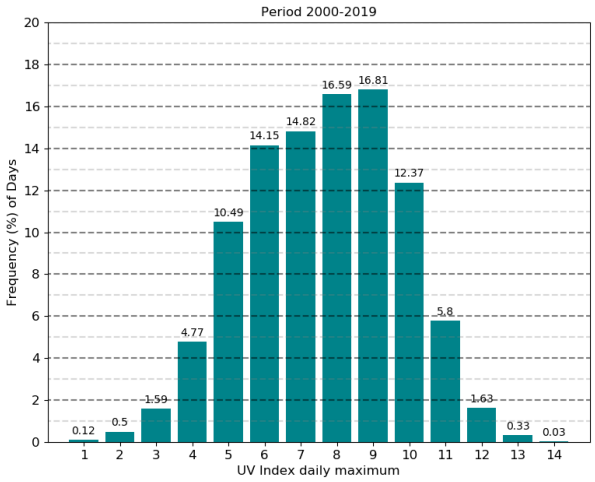

Figure 2: Frequency distribution of maximum daily UV Index values in Mexico city during 2000 -2019.

Figure 3 shows the diurnal variation of the UVI for several specific cloud-free days, for different seasons and several locations. Although the stations are all within a 25 km radius, substantial differences among them are notable. The differences are particularly evident in the afternoons, suggesting that their origin is not related to calibration differences between the instruments. Photographs of the locations also indicate that shadowing from nearby structures is not an issue. It is more likely that local differences in air pollution, particularly aerosols, are the cause of this variability. Previous studies (e.g., (Castro et al., 2001; Palancar et al., 2013)) have shown that surface UV radiation in Mexico City is attenuated significantly by aerosols. The measurements shown in Figure 3 are consistent with increasing pollution during the course of the day, with highest aerosol loading (and highest variability) attained in the afternoon. Further support for the role of pollution in suppressing the UVI comes from the observation made at Santa Fe (SFE) which in Fig. 3 are seen to be systematically higher, e.g. by over 10% in autumn afternoons, compared to the other stations. The SFE station is located at 2600 m asl, approximately 300 m higher than Mexico City downtown, and so avoids a substantial fraction of the polluted MCMA boundary layer. It is expected to have higher values of the UVI, in agreement with the observations.

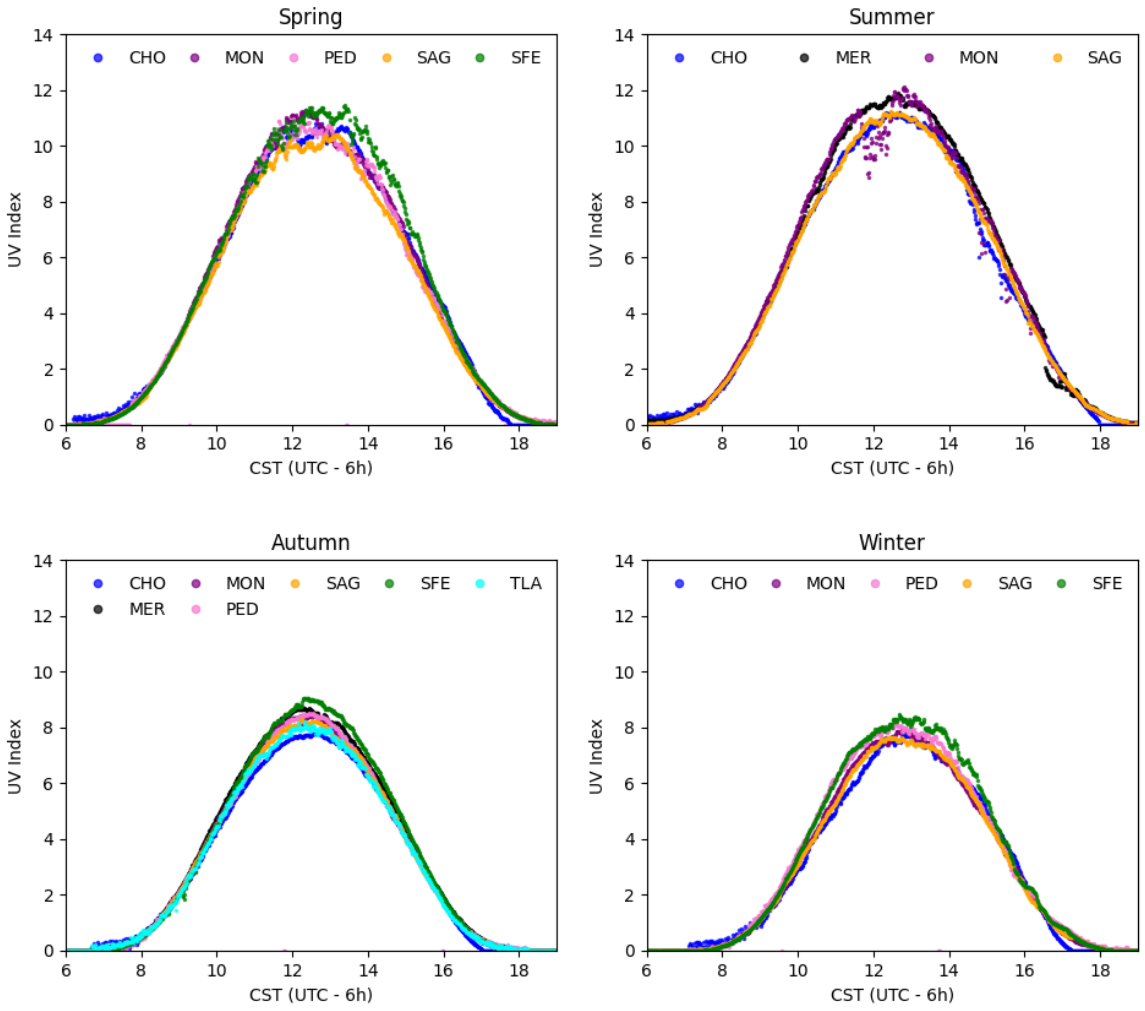

Figure 3: UV Index measured over MCMA by SIMAT stations each minute along the day under cloudless conditions for the seasons and dates (month/day/year): Spring (04/20/2018), Summer (06/04/2018), Autumn (11/13/2018) and Winter (02/02/2018).

Based on ground measurements analysis under all sky conditions we make an assessment of the values reached around solar noon. From daily $UVI_{\max}$, the monthly averages ($\overline{UVI_m}$) and Standard Deviations (SD) were calculated. The `Simple Moving Average` function from `Python` was applied by quarter and a linear fit along the two decades was determined (Figure 4a). The linear equation has a slope m_{UVI} of 0.06 per year and the y-intercept (year 2000) has a UVI value of 8.5. For the sake of representing an annual behavior, the average, the median, SD, maximum and minimum of the UV Index were obtained (Figure 4b). The maximum and minimum monthly mean of the UV Index were 10.6 (in May) and 6.5 (in November), respectively.

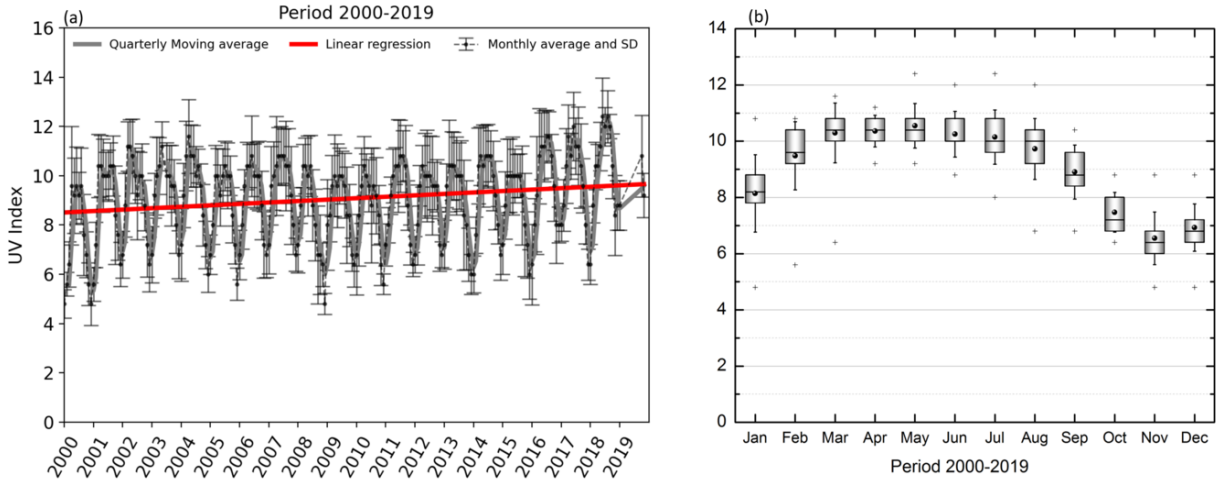

Figure 4: (a) Moving average function (gray curve) quarterly applied to monthly UV Index and SD (black dots and dash line) and its linear fit (red line). (b) Boxplot of monthly UV Index in the period 2000-2019: median (central bold line), average (black dot), 25^{th} and 75^{th} percentiles (box edges), Standard Deviation (the whiskers) and the minimum and maximum values(plus sign).

In January the median and mean UVI values are near 8 (see Fig. 4b). However, the UVI values and SD seems to be flattened (in the range 10-11) from March to August and decreasing to November (rainy period) with a slight rise on December. The rather low monthly UV Index values, may be a consequence of averaging measurements in presence of clouds and/or significant pollution. Both depend on time of the year, with a cool dry season from November to February, warm dry March-April-May, and a rainy season from June to October. In addition to urban aerosol pollution sources, biomass burning for agriculture and wood cooking also contribute to poor air quality in the MCMA (Retama et al., 2015). In the warm season, faster photochemical oxidant formation, dust, and biomass burning all contribute to strong aerosol loading. In rainy months, UV Index values are lower due to the presence of clouds.

For assessing the influence of the aerosols and criteria pollutants in the UV Index, we processed the PM_{10}, CO, NO_2, O_3 and AOD_{340} ground-based measurements carried out at the stations mentioned in Table 2. From daily measurements from 11h to 14h CST the annual mean of PM_{10}, CO, NO_2, O_3 were calculated. For the case of the AOD_{340}, the measurements along of the day were averaged. Figure 5 shows the trends of the annual values from 2000 to 2019. On the other hand, to estimate the percentage change per year ($\epsilon\,(\%)$), the slope (m_X) of the linear fit and the average in all period ($\overline{X}_{2000-2019}$) were used. In the case of the UVI percentage change was 0.66 % per year. In the same way, Table 3 shows the values corresponding to PM_{10}, CO, NO_2, O_3 and AOD_{340}.

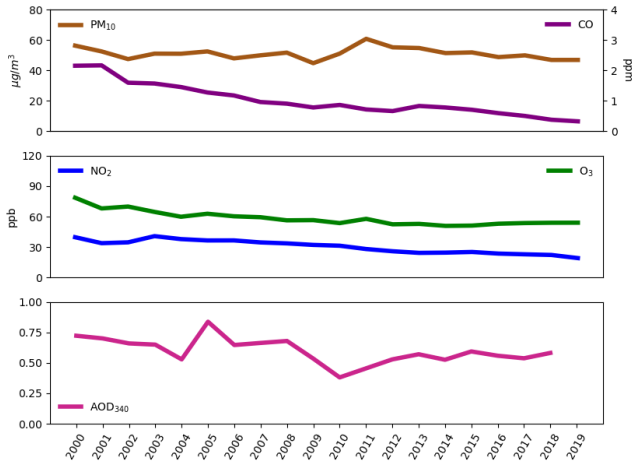

Figure 5: Air quality trends for the period 2000-2019 in Mexico City Metropolitan Area from annual averages obtained between 11h to 14h CST every day: PM_{10} (brown curve), CO (purple curve), NO_2 (blue curve), O_3 (green curve) and AOD_{340} (pink curve).

Policies aimed on the improvement of air quality simultaneously with urban and industrial development have taken place in the last years (Molina et al., 2009). Stephens et al (2008) determined the monthly variation of the concentrations of PM_{10} in the morning (between 7-12h CTS) and O_3 in the afternoon (from 11h to 17h CTS) for the years 2001–2007 with a negative trend (Stephens et al., 2008). These results revel that the decreasing of criteria pollutants could be the cause of the slight increase in the UV index trend. Nevertheless, MCMA has a large period under typical cloudiness days or wet season, in general from June to November.

Name	m_X	$\overline{X}_{2000-2019}$	$\epsilon(\%)$
UVI	0.06	9.085	0.66
PM_{10}	-0.1196	51.11	-0.23
CO	-0.0835	1.02	-8.18
NO_2	-1.04	30.35	-3.43
O_3	-1.046	58.48	-1.79
AOD_{340}	-0.01	0.60	-1.67

Table 3: UV Index and criteria pollutants: slope from linear fit, average 2000-2019 in units of $\mu g/m^3(PM_{10})$, ppm (CO), ppb (NO_2 and O_3) and dimensionless (UV Index and AOD_{340}) and annual percentage change (%/year)

A fundamental issue is to establish the clouds influence on the mean UV Index values. Cloudy days are frequent almost all year in MCMA. The attenuation on $UVI_{\max}$ by clouds could also be predominant out of the rainy period. However, a gap in our knowledge is to discriminate cloudy days only using hourly UV Index measured in situ. The Radiative Cloud Factor measurements by OMI-Aura/NIVR-FMI-NASA satellite instrument was extracted for the Mexico City coordinates. Figure 6a depicts the daily Cloud Factor (5844 observations) recorded from 2004 to 2019 period. It revealed that cloud cover regularly appears in part of the warm dry and rainy seasons, and is frequent the rest of the months.

Moreover, to incorporate satellite information about the total ozone column (TOC) is fundamental for understanding the UV Index levels. Regarding the cold dry period (December to February) TOMS-EP/NASA

and OMI-Aura/NIVR-FMI-NASA instruments estimated the lowest clouds coverage as well as the lowest TOC (Figure 6b). Conversely, higher ozone levels were registered from April to September.

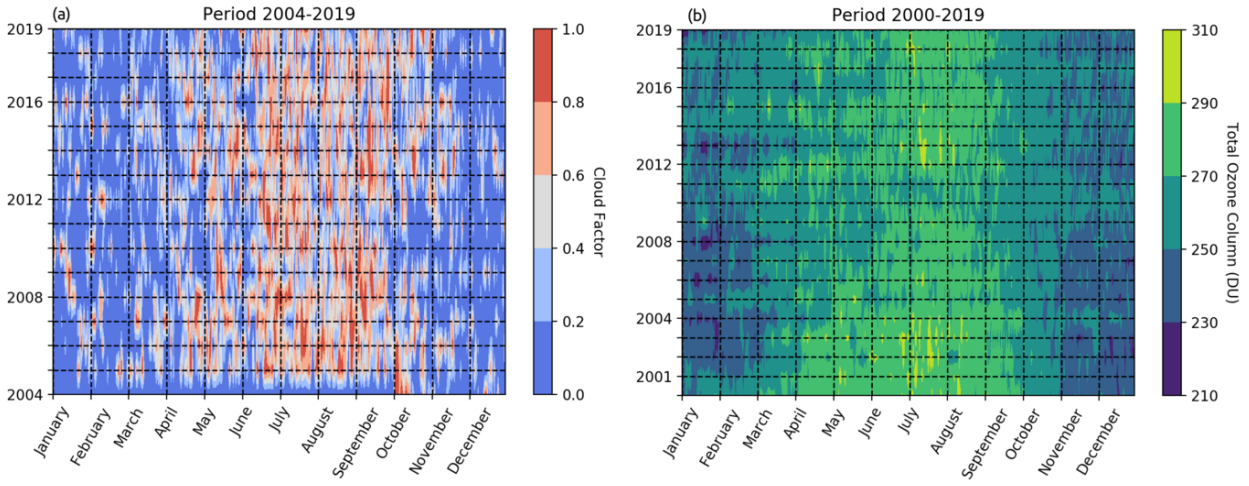

Figure 6: Satellite data over Mexico City: (a) Cloud Factor OMI-Aura/NIVR-FMI-NASA between 2004-2019 and (b) Total Ozone Column from TOMS-EP/NASA and OMI-Aura/NIVR-FMI-NASA in the periods 2000-2003 and 2004-2019, respectively.

To compare the ground-base measurements at solar noon, the UV Index measured by OMI-Aura/NIVR-FMI-NASA were mapped. Figure 7 represents the satellite UV Index data from 2005 to 2019 (there was no previous data in the analyzed period). As can be seen, the levels are higher than the monthly averages shown in Figure 4 (where the UVI maximum values barely exceed 11). From the middle of January to mid-November, the satellite UV Index varies from 8 up to about 15 ($UVI_{\max} = 14.9$). In particular, values equal or larger than 11, corresponding to the *Extreme* qualification for the UV index given by WHO, are commons from April to September.

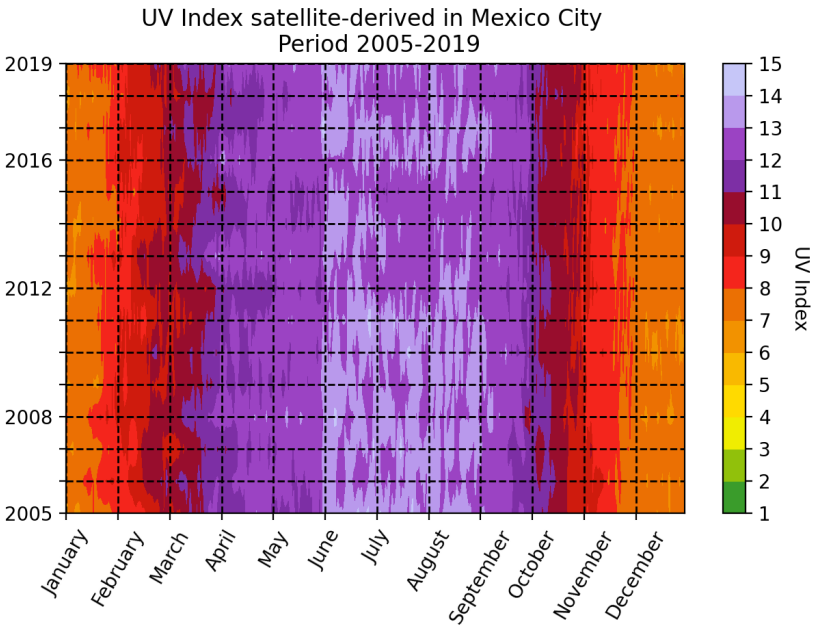

Figure 7: UV Index recorded by OMI-Aura/NIVR-FMI-NASA, from 2005 to 2019.

The UVI derived from satellite observations is seen to be systematically larger than the mean UVI values measured at the ground. This is to some extent expected, since satellites fail to resolve local clouds and aerosols, particularly near surface levels. To examine this over-estimation in more detail, we selected a subset of the ground-based data that included only the maximum value from all stations and all years of measurement, for each hour and day of the year. The result for the compilation of this $UVI_{\max}$ is illustrated in Figure 8. It can be seen that $UVI_{\max} \geq 8$ is very frequent at solar noon, as was seen in Figure 2, corresponding to the daily maximum near noon. The highest $UVI_{\max}$ recorded in the period 2000-2019 was 14.9, which is consistent with the maximum values obtained from satellite observations.

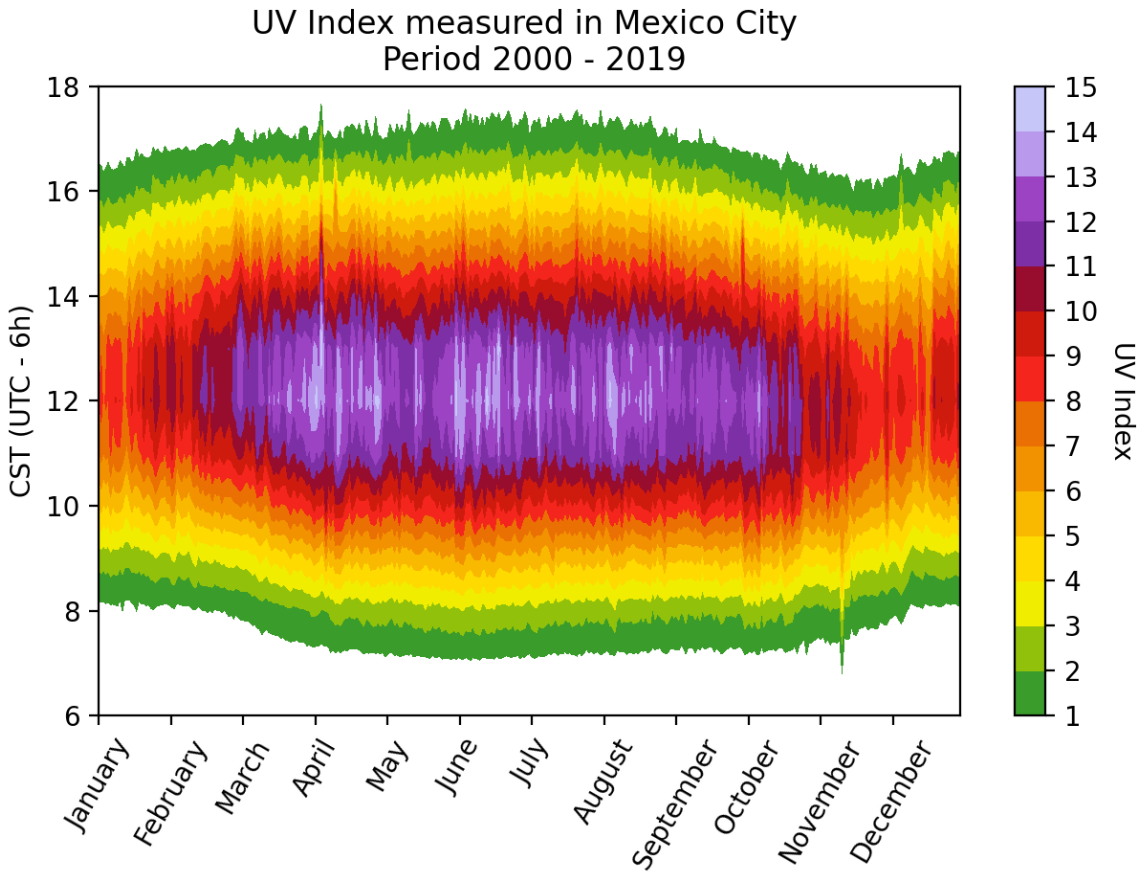

Figure 8: The highest UV Index values recorded during 2000-2019, for each day of the year and each hour of the day. Selected from SIMAT observations in Mexico City.

However, this comparison also suggests that satellite data estimate may be biased to low values under some conditions. The most noticeable difference is in December, when the $UVI_{\max}$ in situ are between 8-11 and satellite data ranging from 6 to 8.

A visual screening process was applied to the ground measurements to separate cloudless and cloudy conditions, as automated methods are still challenging (Badosa et al., 2014; Wild et al., 2019). In spite of the lack of information about the presence of clouds during the day, the data acquired each minute in the period 2016-2018 were a great identification tool. The measurements behavior minute by minute was used to recognize clear sky days. As expected, the monthly averages UV Index under cloudless sky were higher than $\overline{UVI}_m$, probably due to the clouds absence.

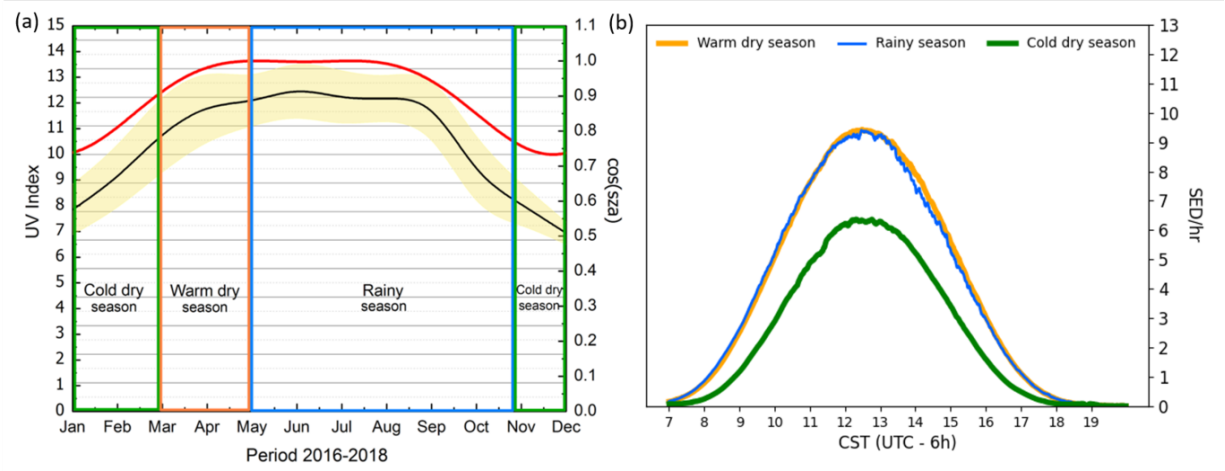

Figure 9: Seasonal variability of the UV Index from ground measurement under cloudless sky in cold dry season (green), warm dry season (orange) and rainy season (blue) for: (a) Interpolation of the monthly mean UV Index (and respective SD in wide yellow bands) at solar noon in the period 2016-2018 (black curve), and cos(sza) at solar noon (red curve) and (b) Daily averages of the SED/hr along the hours of the day, for each season.

The SIMAT publishes a recommendation of protection according to the measured UVI. In this way, it would be more convenient to estimate in term of SED/hr and then, to derive the exposure times. The H_{er} expressed as function of time can be obtained (by combing Eqs. 1 and 2)

$$\frac{SED}{hr} = 0.9UVI. \tag{3}$$

As is indicated in Figure 9a, the interpolation of the UV Index (and corresponding SED/hr) at solar noon under clear sky, revels that these levels match better with the $UVI_{\max}$ values measured over the network (see Figure 8) and the highest UV Index value of 12.6 (11.3 SED/hr) in June. Additionally, the SED/hr under all clear sky days were averaged for the three seasons: cold dry, warm dry and rainy, as is shown in Figure 9b. The warm dry and rainy seasons have a behavior almost coincident. Few data under clear sky were detected between September and October (part of the rainy season) being a negligible contribution on total average just when the UV Index decrease. Nevertheless, the daily asymmetries around solar noon shown in Figure 3 could be caused by criteria gases and aerosol. An additional comparison between AOD ground-based measurements and derived data from model (Castro et al., 2001; Cabrera et al., 2012; Palancar et al., 2013) are needed to confirm this hypothesis. However, the main reason for the seasonal variation of the cloud-free UVI is not due to aerosols, but rather simply to the annual cycle of the solar zenith angle, the cosine of which is also plotted in Fig. 9a and is seen to correlate well with the UVI.

As was mentioned in the Introduction, the phototypes III and IV are the most frequents in Mexican inhabitants. The code in `Python` was executed to compute the accumulate doses H_{er} by means of Equation 2. Particularly, the solar exposure time as function of the local hour (considering only clear sky days in the period 2016-2018) were estimated for the skin types III and IV by means the repetitive operation until reach 3.0 SED and 4.5 SED, respectively. Figure 10 illustrates the result of exposure time to accumulate the corresponding H_{er} for each phototype.

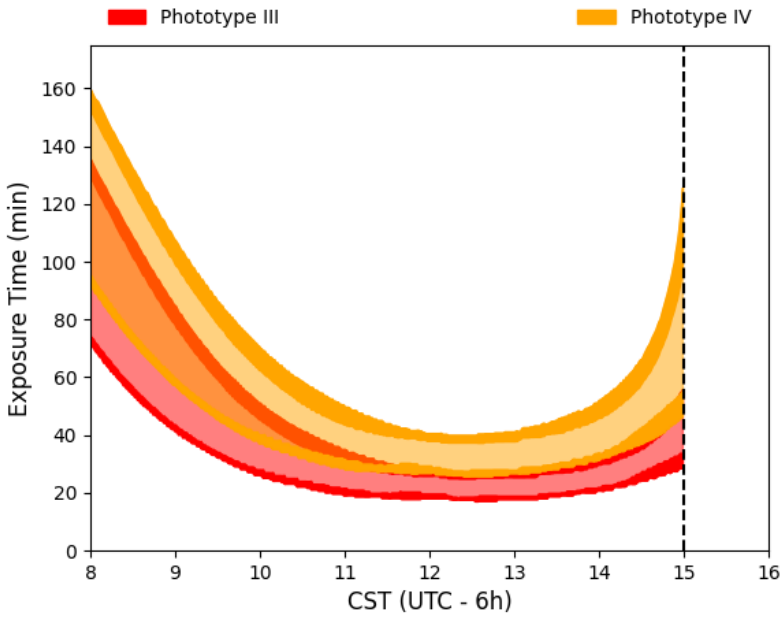

Figure 10: Solar Exposure Time along of the hours of the day for typical skin type of the Mexican population to accumulate H_{er}: 3.0 SED for phototype III (red curves) and and 4.5 SED for phototype IV (yellow curves). Enveloping curves represent the limit times in summer (lower curve) and winter (higher curve). Dotted lines at 15h CST detail the final time when the minimal erythemal dose cannot be reached.

The upper and lower wide curves are associated to measurements carried out in summer and winter seasons and the areas contain the exposure times between spring and autumn. The asymptote at 15h CTS represents that it will not be possible to achieve the MED after this hour. The representation along the hours shows that the exposure time range was narrower, since in this case only clear sky measurements we considered.

Conclusion

The aim of this study was characterize the UV Index reached over Mexico City Metropolitan Area in the last 20 years. The location of this megacity is in a region prone to achieve high values of UV Index (Tanskanen et al., 2006; Zaratti et al., 2014). In spite of Mexico City high altitude (2240 m asl) the ultraviolet irradiance is lower than in Colima (485 m asl), a relatively pollution-free city and placed at about the same latitude (Galindo et al., 1995). The $\overline{UVI}_m$ at solar noon reaches up to 10.6 obtained under all sky conditions (see Figure 4). In contrast, UV Index from satellite data (Figure 7) and the highest $UVI_{\max}$ ground-based values were 14.9 (in Figure 8), both in *Extreme* qualification range of WHO (WHO, 2002). The high aerosols concentration and smog photochemistry products may affect the solar radiation reaching the surface (Castro et al., 2001; Palancar et al., 2013). Also the existence of cloud coverage almost all year round can be partially responsible for the not as high as expected UV index values for Mexico city. In the period 2000-2019 the criteria pollutants trends: PM_{10}, CO, NO_2, O_3 and AOD_{340} were negatives. However the $\overline{UVI}_m$ at solar noon under all sky conditions are in the *High, Very High and Extreme* ranges ($\overline{UVI} \geq 6$) during all months of the year (see Figures 4, 7 and 8). The few articles existing about solar radiation in this city have either been short-term studies or have not focused on UV irradiance affecting health skin. In this work, a code in `Python` was created to analyze the complete database at different scales of time (minute, hours, days and years) calculating the averages and the maximums UV Index as well and its trend. One part of the script was extended to the management and determination of the exposure times corresponding to the threshold

erythemal dose. The levels of UV Index at noon in the period 2000 to 2019 over MCMA show a trend of 0.66 % per year with respect to the mean. This trend is within the range of the results published by Herman (2010) about erythemal irradiance trend from 1979 to 2008 derived from satellite data (between -1.7% to 2.0% annually) in the latitudinal range of Mexico City. The current study also contributes to the determination of the solar exposure time as a limit to avoid sunburn, considering the phototypes more frequent of the inhabitants of the Mexico City. Regarding to skin color to define the sensibility, imprecise terminology such as 'ethnic skin' and 'Hispanic skin' accentuates the problem of sparse data and hides relevant characteristics. There are discrepancies between the MED values defined for each phototype (Fitzpatrick, 1988; Sanclemente et al., 2008; Pérez et al., 2014; Lehmann et al., 2019; Cadet et al., 2019). The definition of the colors gradient and the descriptive numbers associated to the phototypes should always be clear and specific. An essential element is assuming ethnic diversity. The threshold erythemal dose for each phototype is fundamental to awareness of the photoprotection. The photoprotection needs to be promoted with properly communication about the risk and skin care. This premise would help to demystify the perception about the fact that the darker skins can not have sunburn or are exempt to develop skin-cancer (Castanedo-Cazares et al., 2006). Prevention and timely diagnosis continue to be the main strategy to reduce the incidence and impact of skin cancer (Pinedo et al., 2009; Alfaro-Sánchez et al., 2016). This study highlights the importance of knowing the UV Index levels and the maximum exposure times to avoid damage. The prevention campaigns may be accompanied by recommendations associated with typical customs of the country, such as the use of hats and long-sleeved shirts when they work or perform recreational activities in outdoors conditions.

Acknowledgements

We wish to acknowledge the SEDEMA members, institution that belongs to the Mexico City Government. We would like to express special gratitude to Q. Armando Retama for his great job in the management data network and constant advisory. Adriana Ipiña would like to extend her thanks to Dirección General de Personal Académico, Universidad Nacional Autónoma de México (DGAPA-UNAM) for the postdoctoral fellowship at Centro de Ciencias de la Atmósfera of the UNAM. Rubén D Piacentini wishes to thank CONICET and National University of Rosario, Argentina, for their partial support to the present work. The National Center for Atmospheric Research is sponsored by the National Science Foundation.

References

Acosta, L.R., Evans, W.F.J., 2000. Design of the Mexico City UV monitoring network: UV-B measurements at ground level in the urban environment. Journal of Geophysical Research: Atmospheres 105, 5017–5026. https://doi.org/10.1029/1999jd900250

Alfaro-Sánchez, A., García-Hidalgo, L., Casados-Vergara, R., Rodríguez-Cabral, R., Piña-Osuna, A.K., Sánchez-Ramos, A., 2016. Cáncer de piel. Epidemiología y variedades histológicas, estudio de cinco años en el noreste de México. Dermatol Rev Mex. 60(2).

Badosa, J., Calbó, J., Mckenzie, R., Liley, B., González, J.A., Forgan, B., Long, C.N., 2014. Two methods for retrieving UV index for all cloud conditions from sky imager products or total SW radiation measurements.. Photochem Photobiol 90, 941–51.

Bino, S.D., Bernerd, F., 2013. Variations in skin colour and the biological consequences of ultraviolet radiation exposure. British Journal of Dermatology 169, 33–40. https://doi.org/10.1111/bjd.12529

Braslavsky, S.E., 2007. Glossary of terms used in photochemistry 3rd edition (IUPAC Recommendations 2006). Pure and Applied Chemistry 79, 293–465. https://doi.org/10.1351/pac200779030293

CIE, 2014. Rationalizing Nomenclature for UV dose and effects on humans. The International Commission on Illumination and World Meteorological Organization.

Cabrera, S., Ipiña, A., Damiani, A., Cordero, R.R., Piacentini, R.D., 2012. UV index values and trends in Santiago Chile (33.5°S) based on ground and satellite data. Journal of Photochemistry and Photobiology B: Biology 115, 73–84. https://doi.org/10.1016/j.jphotobiol.2012.06.013

Cadet, J.-M., Bencherif, H., du Preez, D.J., Portafaix, T., Sultan-Bichat, N., Belus, M., Brogniez, C., Auriol, F., Metzger, J.-M., Ncongwane, K., Coetzee, G.J.R., Wright, C.Y., 2019. Solar UV Radiation in Saint-Denis La Réunion and Cape Town, South Africa: 10 years Climatology and Human Exposure Assessment at Altitude. Atmosphere 10, 589. https://doi.org/10.3390/atmos10100589

Castanedo-Cazares, J.P., Torres-Álvarez, B., Medellín-Pérez, M.E., Aguilar-Hernández, G.A., Moncada, B., 2006. Conocimientos y actitudes de la población mexicana con respecto a la radiación solar. Gaceta Médica de México 142.

Castanedo-Cázares, J.P., Torres-Álvarez, B., Ondarza, S.S., Pérez, A.E., Moscoso, A.G., 2012. Estimación del tiempo de exposición solar para quemadura en población mexicana. Gaceta Médica de México 148.

Castro, T., Madronich, S., Rivale, S., Muhlia, A., Mar, B., 2001. The influence of aerosols on photochemical smog in Mexico City. Atmospheric Environment 35, 1765–1772. https://doi.org/10.1016/s1352-2310(00)00449-0

Cede, A., Luccini, E., Nuñez, L., Piacentini, R.D., Blumthaler, M., 2002. Monitoring of erythemal irradiance in the Argentine ultraviolet network. Journal of Geophysical Research 107. https://doi.org/10.1029/2001jd001206

Corr, C.A., Krotkov, N., Madronich, S., Slusser, J.R., Holben, B., Gao, W., Flynn, J., Lefer, B., Kreidenweis, S.M., 2009. Retrieval of aerosol single scattering albedo at ultraviolet wavelengths at the T1 site during MILAGRO. Atmospheric Chemistry and Physics 9, 5813–5827. https://doi.org/10.5194/acp-9-5813-2009

Cuevas, A.G., Dawson, B.A., Williams, D.R., 2016. Race and Skin Color in Latino Health: An Analytic Review. American Journal of Public Health 106, 2131–2136. https://doi.org/10.2105/ajph.2016.303452

Dickerson, R.R., 1997. The Impact of Aerosols on Solar Ultraviolet Radiation and Photochemical Smog. Science 278, 827–830. https://doi.org/10.1126/science.278.5339.827

Doran, J.C., Abbott, S., Archuleta, J., Bian, X., Chow, J., Coauthors, 1998. The IMADA-AVER Boundary Layer Experiment in the Mexico City Area. Bull. Amer. Meteor. Soc. 79.

ENADIS, 2017. Encuesta Nacional sobre Discriminación. CONAPRED and INEGI.

Finlayson-Pitts, B.J., Pitts, J.N., 2000. Chemistry of the Upper and Lower Atmosphere. Elsevier. https://doi.org/10.1016/b978-012257060-5/50000-9

Fioletov, V.E., Kimlin, M.G., Krotkov, N., McArthur, L.J.B., Kerr, J.B., Wardle, D.I., Herman, J.R., Meltzer, R., Mathews, T.W., Kaurola, J., 2004. UV index climatology over the United States and Canada from ground-based and satellite estimates. Journal of Geophysical Research: Atmospheres 109, n/a–n/a. https://doi.org/10.1029/2004jd004820

Fitzpatrick, T.B., 1974. Sunlight and man: An introduction to the problem of normal and abnormal of responses man's skin to solar radiation. University of Tokyo Press.

Fitzpatrick, T.B., 1988. The validity and practicality of sun-reactive skin types I through VI.. Arch Dermatol 124, 869–71.

Galindo, I., Castro, S., Valdes, M., 1991. Satellite derived solar irradiance over Mexico. Atmósfera 4.

Galindo, I., Frenk, S., Bravo, H., 1995. Ultraviolet Irradiance over Mexico City. Journal of the Air & Waste Management Association 45, 886–892. https://doi.org/10.1080/10473289.1995.10467419

Goering, C.D., 2005. Simultaneous retrievals of column ozone and aerosol optical properties from direct and diffuse solar irradiance measurements. Journal of Geophysical Research 110. https://doi.org/10.1029/2004jd005330

Herman, J.R., 2010. Global increase in UV irradiance during the past 30 years (1979–2008) estimated from satellite data. Journal of Geophysical Research 115. https://doi.org/10.1029/2009jd012219

Holben, B.N., Eck, T.F., Slutsker, I., Tanré, D., Buis, J.P., Setzer, A., Vermote, E., Reagan, J.A., Kaufman, Y.J., Nakajima, T., Lavenu, F., Jankowiak, I., Smirnov, A., 1998. AERONET—A Federated Instrument Network and Data Archive for Aerosol Characterization. Remote Sensing of Environment 66, 1–16. https://doi.org/10.1016/s0034-4257(98)00031-5

Jurado-Santa-Cruz, F., Medina-Bojórquez, A., Gutiérrez-Vidrio, R.M., Ruiz-Rosillo, J.M., 2011. Prevalencia del cáncer de piel en tres ciudades de México. Rev Med Inst Mex Seguro Soc. 49(3).

Lancer, H.A., 1998. Lancer Ethnicity Scale (LES). Lasers Surg Med 22, 9.

Larkö, O., Diffey, B.L., 1983. Natural UV-B radiation received by people with outdoor, indoor, and mixed occupations and UV-B treatment of psoriasis.. Clin Exp Dermatol 8, 279–85.

Lehmann, M., Pfahlberg, A.B., Sandmann, H., Uter, W., Gefeller, O., 2019. Public Health Messages Associated with Low UV Index Values Need Reconsideration. International Journal of Environmental Research and Public Health 16, 2067. https://doi.org/10.3390/ijerph16122067

Leighton, P.A., 1961. Photochemistry of Air Pollution, in: . Elsevier, pp. v–vi. https://doi.org/10.1016/b978-0-12-442250-6.50004-3

Luccini, E., Cede, A., Piacentini, R., Villanueva, C., Canziani, P., 2006. Ultraviolet climatology over Argentina. Journal of Geophysical Research 111. https://doi.org/10.1029/2005jd006580

MacKie, R.M., 2000. Effects of Ultraviolet Radiation on Human Health. Radiation Protection Dosimetry 91, 15–18. https://doi.org/10.1093/oxfordjournals.rpd.a033186

Madronich, S., 1993. The Atmosphere and UV-B Radiation at Ground Level, in: Environmental UV Photobiology. Springer US, pp. 1–39. https://doi.org/10.1007/978-1-4899-2406-3_1

Makgabutlane, M., and Caradee Wright, and, and, 2015. Real-time measurement of outdoor worker's exposure to solar ultraviolet radiation in Pretoria South Africa. South African Journal of Science 111. https://doi.org/10.17159/sajs.2015/20140133

Marcheco-Teruel, B., Parra, E.J., Fuentes-Smith, E., Salas, A., Buttenschøn, H.N., Demontis, D., Torres-Español, M., Marín-Padrón, L.C., Gómez-Cabezas, E.J., Álvarez-Iglesias, V., Mosquera-Miguel, A., Martínez-Fuentes, A., Ángel Carracedo, Børglum, A.D., Mors, O., 2014. Cuba: Exploring the History of Admixture and the Genetic Basis of Pigmentation Using Autosomal and Uniparental Markers. PLoS Genetics 10, e1004488. https://doi.org/10.1371/journal.pgen.1004488

Matsumoto, Y., Valdés, M., Urbano, J.A., Kobayashi, T., López, G., Peña, R., 2014. Global Solar Irradiation in North Mexico City and Some Comparisons with the South. Energy Procedia 57, 1179–1188. https://doi.org/10.1016/j.egypro.2014.10.105

Meinhardt, M., Krebs, R., Anders, A., Heinrich, U., Tronnier, H., 2008. Wavelength-dependent penetration depths of ultraviolet radiation in human skin.. J Biomed Opt 13, 044030.

Miller, S.A., Coelho, S.G., Miller, S.W., Yamaguchi, Y., Hearing, V.J., Beer, J.Z., 2012. Evidence for a new paradigm for ultraviolet exposure: a universal schedule that is skin phototype independent.. Photodermatol Photoimmunol Photomed 28, 187–95.

Moldovan, H.R., Wittlich, M., John, S.M., Brans, R., Tiplica, G.S., Salavastru, C., Voidazan, S.T., Duca, R.C., Fugulyan, E., Horvath, G., Alexa, A., Butacu, A.I., 2020. Exposure to solar UV radiation in outdoor

construction workers using personal dosimetry. Environmental Research 181. https://doi.org/10.1016/j.envres.2019.108967

Molina, L.T., Kolb, C.E., de Foy, B., Lamb, B.K., Brune, W.H., Jimenez, J.L., Ramos-Villegas, R., Sarmiento, J., Paramo-Figueroa, V.H., Cardenas, B., Gutierrez-Avedoy, V., Molina, M.J., 2007. Air quality in North America's most populous city – overview of the MCMA-2003 campaign. Atmospheric Chemistry and Physics 7, 2447–2473. https://doi.org/10.5194/acp-7-2447-2007

Molina, L.T., Madronich, S., Gaffney, J.S., Apel, E., de Foy, B., Fast, J., Ferrare, R., Herndon, S., Jimenez, J.L., Lamb, B., Osornio-Vargas, A.R., Russell, P., Schauer, J.J., Stevens, P.S., Volkamer, R., Zavala, M., 2010. An overview of the MILAGRO 2006 Campaign: Mexico City emissions and their transport and transformation. Atmospheric Chemistry and Physics 10, 8697–8760. https://doi.org/10.5194/acp-10-8697-2010

Molina, L.T., de Foy, B., Vázquez-Martínez, O., Páramo-Figueroa, V.H., 2009. Air Quality, Weather and Climate in Mexico City. Bulletin WMO 58 (1).

Palancar, G.G., Lefer, B.L., Hall, S.R., Shaw, W.J., Corr, C.A., Herndon, S.C., Slusser, J.R., Madronich, S., 2013. Effect of aerosols and NO_2 concentration on ultraviolet actinic flux near Mexico City during MILAGRO: measurements and model calculations. Atmospheric Chemistry and Physics Discussions 13. https://doi.org/10.5194/acp-13-1011-2013

Parra, R., Cadena, E., Flores, C., 2019. Maximum UV Index Records (2010–2014) in Quito (Ecuador) and Its Trend Inferred from Remote Sensing Data (1979–2018). Atmosphere 10, 787. https://doi.org/10.3390/atmos10120787

Parrish, D.D., Singh, H.B., Molina, L., Madronich, S., 2011. Air quality progress in North American megacities: A review. Atmospheric Environment 45, 7015–7025. https://doi.org/10.1016/j.atmosenv.2011.09.039

Pinedo, J.L., Castaneda, R., McBride, L.E., Davila, I., Mireles, F., Ríos, C., 2009. Estimates of the Skin Cancer Incidence in Zacatecas, México. The Open Dermatology Journal 3, 58–62. https://doi.org/10.2174/1874372200903010058

Pérez, F.A., Aguilera, J., Aguilera, P., de, A.D., Barnadas, M.A., de, C.X., Carrrascosa, J.M., de, G.A.M.V., Gardeazábal, J., Giménez-Arnau, A., Lecha, M., Lorente, J., Martínez-Lozano, J.A., Rodríguez, G.M.T., Sola, Y., Utrillas, M.P., 2014. Determination of minimal erythema dose and anomalous reactions to UVA radiation by skin phototype.. Actas Dermosifiliogr 105, 780–8.

Quiñones, A., Almanza, R., 2014. Modeling Ultraviolet Radiation for Mexican Conditions. Energy Procedia 57, 1220–1226. https://doi.org/10.1016/j.egypro.2014.10.110

Retama, A., Baumgardner, D., Raga, G.B., McMeeking, G.R., Walker, J.W., 2015. Seasonal and diurnal trends in black carbon properties and co-pollutants in Mexico City. Atmospheric Chemistry and Physics 15, 9693–9709. https://doi.org/10.5194/acp-15-9693-2015

Rivas, M., Araya, M.C., Caba, F., Rojas, E., Calaf, G.M., 2011. Ultraviolet light exposure influences skin cancer in association with latitude. Oncology Reports 25. https://doi.org/10.3892/or.2011.1164

Rivas, M., Rojas, E., Araya, M.C., Calaf, G.M., 2015. Ultraviolet light exposure skin cancer risk and vitamin D production. Oncology Letters 10, 2259–2264. https://doi.org/10.3892/ol.2015.3519

Robinson, J.K., Penedo, F.J., Hay, J.L., Jablonski, N.G., 2017. Recognizing Latinos' range of skin pigment and phototypes to enhance skin cancer prevention. Pigment Cell & Melanoma Research 30, 488–492. https://doi.org/10.1111/pcmr.12598

Rouhani, P., Hu, S., Kirsner, R.S., 2008. Melanoma in Hispanic and Black Americans. Cancer Control 15, 248–253. https://doi.org/10.1177/107327480801500308

Sanclemente, G., Zapata, J.-F., García, J.-J., Ángela Gaviria, Gómez, L.-F., Barrera, M., 2008. Lack of correlation between minimal erythema dose and skin phototype in a colombian scholar population. Skin Research and Technology 14, 403–409. https://doi.org/10.1111/j.1600-0846.2008.00306.x

Seinfeld, J.H., Pandis, S.N., 2016. Atmospheric Chemistry and Physics: From Air Pollution to Climate Change. Wiley.

Silva, A.A., 2016. Outdoor Exposure to Solar Ultraviolet Radiation and Legislation in Brazil. Health Physics 110, 623–626. https://doi.org/10.1097/hp.0000000000000489

Staiger, H., Koepke, P., 2005. UV Index forecasting on a global scale. Meteorologische Zeitschrift 14, 259–270. https://doi.org/10.1127/0941-2948/2005/0029

Stephens, S., Madronich, S., Wu, F., Olson, J.B., Ramos, R., Retama, A., Muñoz, R., 2008. Weekly patterns of México City's surface concentrations of CO NOx PM10and O3during 1986–2007. Atmospheric Chemistry and Physics 8, 5313–5325. https://doi.org/10.5194/acp-8-5313-2008

Tanskanen, A., Krotkov, N.A., Herman, J.R., Arola, A., 2006. Surface ultraviolet irradiance from OMI. IEEE Transactions on Geoscience and Remote Sensing 44, 1267–1271. https://doi.org/10.1109/tgrs.2005.862203

Taylor, S.C., Arsonnaud, S., Czernielewski, J., Group, H.S.S., 2005. The Taylor Hyperpigmentation Scale: A new visual assessment tool for the evaluation of skin color and pigmentation. Journal of the American Academy of Dermatology 52, P170. https://doi.org/10.1016/j.jaad.2004.10.691

Tejeda-Martínez, A., Jáuregui-Ostos, E., 2005. Surface energy balance measurements in the México City region: a review. Atmósfera 18.

Torres, V., Herane, M.I., Costa, A., Martin, J.P., Troielli, P., 2017. Refining the ideas of ethnic skin. Anais Brasileiros de Dermatologia 92, 221–225. https://doi.org/10.1590/abd1806-4841.20174846

Tzompa-Sosa, Z.A., Sullivan, A.P., Retama, A., Kreidenweis, S.M., 2017. Contribution of Biomass Burning to Carbonaceous Aerosols in Mexico City during May 2013. Aerosol and Air Quality Research 16, 114–124. https://doi.org/10.4209/aaqr.2015.01.0030

UN, 2014. World urbanization prospects. United Nations. https://doi.org/10.18356/527e5125-en

Utrillas, M.P., Marín, M.J., Esteve, A.R., Salazar, G., Suárez, H., Gandía, S., Martínez-Lozano, J.A., 2018. Relationship between erythemal UV and broadband solar irradiation at high altitude in Northwestern Argentina. Energy 162, 136–147. https://doi.org/10.1016/j.energy.2018.08.021

WHO, 2002. Global Solar UV Index: A Practical Guide.

Whiteman, C.D., Zhong, S., Bian, X., Fast, J.D., Doran, J.C., 2000. Boundary layer evolution and regional-scale diurnal circulations over the and Mexican plateau. Journal of Geophysical Research: Atmospheres 105, 10081–10102. https://doi.org/10.1029/2000jd900039

Wild, M., Hakuba, M.Z., Folini, D., Dörig-Ott, P., Schär, C., Kato, S., Long, C.N., 2019. The cloud-free global energy balance and inferred cloud radiative effects: an assessment based on direct observations and climate models.. Clim Dyn 52, 4787–4812.

Wolbarsht, M.L., Urbach, F., 1999. The Lancer Ethnicity Scale.. Lasers Surg Med 25, 105–6.

Zaratti, F., Piacentini, R.D., Guillén, H.A., Cabrera, S.H., Liley, J.B., McKenzie, R.L., 2014. Proposal for a modification of the UVI risk scale. Photochem. Photobiol. Sci. 13, 980–985. https://doi.org/10.1039/c4pp00006d

Zhang, Y., Dubey, M.K., Olsen, S.C., Zheng, J., Zhang, R., 2009. Comparisons of WRF/Chem simulations in Mexico City with ground-based RAMA measurements during the 2006-MILAGRO. Atmospheric Chemistry and Physics 9, 3777–3798. https://doi.org/10.5194/acp-9-3777-2009

de Vries, E., Sierra, M., Piñeros, M., Loria, D., Forman, D., 2016. The burden of cutaneous melanoma and status of preventive measures in Central and South America. Cancer Epidemiology 44, S100–S109. https://doi.org/10.1016/j.canep.2016.02.005